REGULAR ARTICLE

Adsorption of transition metal atoms on the NiO(100) surface and on NiO/Ag(100) thin films

**Fabrizio Cinquini · Livia Giordano ·
Gianfranco Pacchioni**

Abstract We have studied the adsorption of Au, Pd, and Pt atoms on the NiO(100) surface and on NiO/Ag(100) thin films using plane wave DFT+U calculations. The scope of this work is to compare the adsorption properties of NiO, a reducible transition metal oxide, with those of MgO, a simple binary oxide with the same crystal structure and similar lattice parameter. At the same time, we are interested in the adsorption characteristics of NiO ultra-thin films (three atomic layers) deposited on Ag(100) single crystals. Also in this case the scope is to compare NiO/Ag(100) with the corresponding MgO/Ag(100) films which show unusual properties for the case of Au adsorption. The results show that the transition metal atoms bind in a similar way on NiO(100) and NiO/Ag(100) films, with Pt, Pd, and Au forming bonds of decreasing strength in this order. No charging effects occur for Au adsorbed on NiO/Ag(100) films, at variance with MgO/Ag(100). The reasons are analyzed in terms of work function of the metal/oxide interface. Possible ways to modify this property by growing alternate layers of MgO and NiO are discussed.

1 Introduction

The study of the adsorption of metal atoms deposited on oxide surfaces is a key step in the understanding their diffusion and aggregation to form small metal particles [1–4]. This is an interesting problem not only in the field of model catalysts

---

F. Cinquini · L. Giordano · G. Pacchioni (✉)
Dipartimento di Scienza dei Materiali,
Università di Milano-Bicocca, Via R. Cozzi, 53,
20125 Milan, Italy
e-mail: gianfranco.pacchioni@unimib.it

[5,6] but also more in general in that of supported metal particles, a class of materials with potential applications for their optical and magnetic properties. To better understand the behavior of metal atoms and clusters deposited on an oxide surface, in the last decade considerable efforts have been devoted to the design of well-defined model systems where the level of complexity is much lower than in real working systems [7–12]. This implies a detailed characterization of the structure and morphology of the oxide support, with particular attention to the presence of point or extended defects, appearance of new phases, or simply of low-coordinated sites. In this respect, ultra-thin oxide films grown on metal substrates offer special advantages as they allow one to use photoelectron spectroscopies or scanning tunneling microscopy to characterize, at an atomic level, the structure of the oxide surface and of the deposited metal nanocluster. Recently it has been found that under particular circumstances, ultra-thin oxide films can behave differently from the corresponding surfaces of bulk oxides [13–20]. For oxide films of few atomic layers, the interaction with the metal substrate can lead to completely different chemistry with respect to the thicker films. Examples in this direction have been reported for films of MgO [14–18], FeO [19], silica [21], and alumina [17]. For instance, gold atoms or clusters deposited on 2–3 layers thick MgO/Ag(100) or MgO/Mo(100) films become negatively charged, with dramatic consequences on the structure and shape of the supported clusters which grow two-dimensional on the thin films and three-dimensional on the thicker films [15,18]. In FeO/Pt(111) films, the modulation of the work function across the oxide provides the basis for using these supports to induce spatial ordering and self-assembling of supported nanoparticles [19]; Au and Pd atoms exhibit completely different adsorption properties on monolayer crystalline silica films grown on Mo(112) [21]: while the Au atoms interact weakly with the film and form small

aggregates even at temperatures as low as 10 K, Pd atoms are small enough to penetrate into the film pores and strongly bind at the interface [22], etc.

Several theoretical studies have been dedicated to the adsorption properties of metal atoms on oxides like MgO and TiO$_2$; much less is known on more complex oxides, in particular transition metal oxides. One oxide surface which has never been studied from this point of view is NiO. The reason is that NiO is a complex material. Standard DFT calculations fail completely in predicting the magnetic insulator character of this oxide, and predict a metallic ground state. The problem can be removed using hybrid functionals or the more pragmatic approach of DFT+U. The DFT+U approach was developed to account for correlation effects arising from the strong on-site Coulomb repulsion and exchange interactions which are essential to properly describe the structure of Mott-Hubbard insulators. It corrects most of the inadequacies connected to the treatment of localized states, but suffers from the dependence of the results on the value of U_{eff}, de facto an empirical parameter. However, few years ago, Cococcioni and De Gironcoli [23] proposed a self-consistent and basis-set independent method for its calculation. Recently we have done a comparative study of the electronic structure of the NiO(100) surface and of NiO/Ag(100) films [24] using an hybrid B3PW functional and localized basis functions, as implemented in the CRYSTAL06 code [25], and the DFT+U approach as implemented in the VASP code [26,27]. The results are encouraging, and we have extended the analysis to the more complex problem of formation of cation and anion vacancies on the NiO(100) surface [28].

In this study we have considered the adsorption of three transition metal atoms, Pd, Pt, and Au, on the NiO(100) surface and on NiO/Ag(100) films. The three atoms are representative of various atomic structures, d^{10}s^{0}Pd, d^{9}s^{1}Pt, and d^{10}s^1 Au. The present study has two main objectives. On one side we want to test the adsorption properties of NiO and compare them with the widely studied MgO surface. In NiO the presence of the Ni^{2+} cation with a partially filled 3d shell and the higher degree of covalency opens the possibility for new bonding mechanisms with respect to the parent MgO surface. The second goal is to compare adsorption of metal atoms, and Au in particular, on NiO(100) and on the corresponding ultra-thin films grown on Ag(100). The unexpected effects discovered on MgO/Mo(100) [14] and MgO/Ag(100) films [16,20] with deposited gold are motivations to explore if similar effects can be present also on the parent NiO/Ag(100) films.

2 Computational details

To reproduce the anti-ferromagnetic and insulating ground state of NiO, the DFT+U approach [29–31] has been adopted.

In DFT+U (either in the LDA or GGA variant) a set of atomic-like orbitals are treated with a new Hamiltonian [29–31], which in the Dudarev approach depends on the difference $U_{eff} = U - J$, where U is a parameter which describes the energy increase for an extra electron on a particular site and J a second parameter which represents the screened exchange energy. For the calculations we used the generalized gradient approximation (GGA) Perdew–Wang 91 (PW91) functional [32] as implemented in the VASP code [26,27] (plane wave basis set, kinetic energy cut off of 400 eV, projected augmented wave (PAW) method [33,34]). As discussed in previous papers [24,28], following what reported by Rohrbach et al. [35] to simulate the NiO electronic structure a value of $U_{eff} = 5.3$ eV ($U = 6.3$ eV and $J = 1$ eV) has been used for the Ni 3d orbitals, which leads to a reasonable value of all parameters of interest.

A 2×2 supercell with a $(3 \times 3 \times 1)$ grid of k-points was used for the slab calculations of NiO films and NiO/Ag(100) interfaces. We adsorbed a metal atom on each 2×2 supercell, which corresponds to a surface coverage $\theta = 0.25$. In both cases the NiO film consists of three atomic layers (3L). The Ag substrate has been represented by five metal layers. The NiO film has been adsorbed only on one side of the Ag slab. All atoms in the oxide films and in the three surface nearest layers of the metal substrate are relaxed until the forces are less than 0.01 eV/Å. For unsupported NiO films the lattice parameter has been fixed to the optimal bulk value; for NiO/Ag(100) films the lattice parameter is that optimized for bulk silver. A vacuum of 18 and 10 Å has been used to separate the NiO(100) and NiO/Ag(100) slabs, respectively. The work function of the system has been obtained as the energy of the vacuum level (determined applying a dipole correction to the unit cell) with respect to the Fermi level of the metal or of the metal/oxide interface.

3 Results and discussion

Before discussing the adsorption of Pd, Pt, and Au atoms on the NiO surface, we summarize the most important properties of NiO(100) and NiO/Ag(100) films. Most of the computed properties of the two systems (supported and unsupported NiO) are similar. In fact, for both MgO and NiO slabs the properties are substantially converged to the bulk ones after 3–4 layers. Experimentally, bulk NiO is an anti-ferromagnetic (AFM) insulator with a band gap, E_g, between 4.0 and 4.3 eV [36–39]. The local magnetic moment of the Ni(111) planes is 1.64–1.77 μ_B at saturation [36,37]. Except for the band gap, these properties are well reproduced by the DFT+U approach which predicts a correct lattice parameter and a magnetisation of about 1.7 μ_B per Ni ion for the AFM phase. The energy gap, about 3 eV, is smaller than in the experiment and in hybrid functional calculations [24].

On the NiO(100) surface the Ni^{2+} ions assume the same $d(z^2)^1 d(x^2 - y^2)^1$ configuration of the bulk (the Ni–O bonds being aligned along the x and y directions), although on the surface the two orbitals are no longer equivalent. Both surface relaxation and surface rumpling are very small [24]. The energy gap, 2.66 eV in DFT+U, is smaller than in the bulk because the film has two surfaces where the atoms are undercoordinated. For the AFM ordering, the magnetization of the inner layers converges to 1.68–1.69 μ_B per Ni ion, similar to the bulk. The top of the valence band is dominated by the O 2p states strongly mixed with the Ni 3d states. The opposite is true for the bottom of the conduction band, which is largely formed by the Ni^{2+} empty 3d states [24].

For 3L NiO films on Ag(100), the Ni ions in the top and inner layers are not perturbed by the bonding at the interface with silver: the magnetization of the Ni ions is slightly quenched only on the NiO layer in direct contact with Ag. The weak adhesion energy can be explained by the analysis of the bonding at the interface. Differently from MgO/Ag(100) [40], it does not arise exclusively from polarization effects, but presents some important covalent contributions [24]. The occurrence of a charge rearrangement at the interface results in a reduction of silver's work function of about 0.4 eV; this is much smaller than in the MgO/Ag(100) interface where the effect is largely determined by a polarization–compression effect (see Ref. [40]). As we will see below, this has important consequences for the adsorption properties.

3.1 Adsorption of Au, Pd and Pt atoms on NiO(100)

We start our discussion with Au. The gold atom has an unpaired electron in the 6s orbital and an extremely high electron affinity (EA), 2.31 eV, one of the largest of the periodic table. For this reason Au atoms adsorbed on oxide surfaces and in particular on point defects like oxygen vacancies can capture one electron and transform into Au^- anions [41]. Several studies have shown that a metal atom deposited on the MgO surface prefers to bind to the oxide anions, where the interaction is stronger. When Au is adsorbed on a clean NiO(100) surface, (Table 1), this is no longer entirely true. We explored extensively the potential energy surface by placing the Au atom on top of O, on top of Ni, or in the hollow site, and optimizing the structure without any symmetry constraint. We found a minimum, corresponding roughly to O-top site with an adsorption energy of 0.90 eV, (Table 1). However, we found that in a constrained hollow geometry, the adsorption energy is only 0.09 eV lower than the O-top one: this suggests we have a region in which the potential energy surface is rather flat. A closer look shows that in the O-top configuration the Au atom is not exactly above the anion, as in the case of MgO, but is tilted by 19° from the surface normal, see Fig. 1. The results found for Au adsorbed on MgO(100) using the same computational approach [14] showed that on

Table 1 Au, Pd, and Pt atoms adsorbed on NiO(100) and NiO/Ag(100)

|	Site	d_{M-Ni}, Å	d_{M-O}, Å	θ (deg)[a]	E_{ads}(eV)
Au/NiO	O-top (tilted)	2.778	2.361	19	0.90
Pd/NiO	O-top (tilted)	2.710	2.078	16	1.60
Pt/NiO	O-top (tilted)	2.677	1.975	18	2.66
Au/NiO/Ag(100)	Ni-top (tilted)	2.527	3.284	6	0.91
	Hollow	2.706	2.731	0	0.95
Pd/NiO/Ag(100)	O-top (tilted)	2.709	2.078	14	1.58
Pt/NiO/Ag(100)	O-top (tilted)	2.714	1.973	13	2.63

[a] Tilt angle from the surface normal
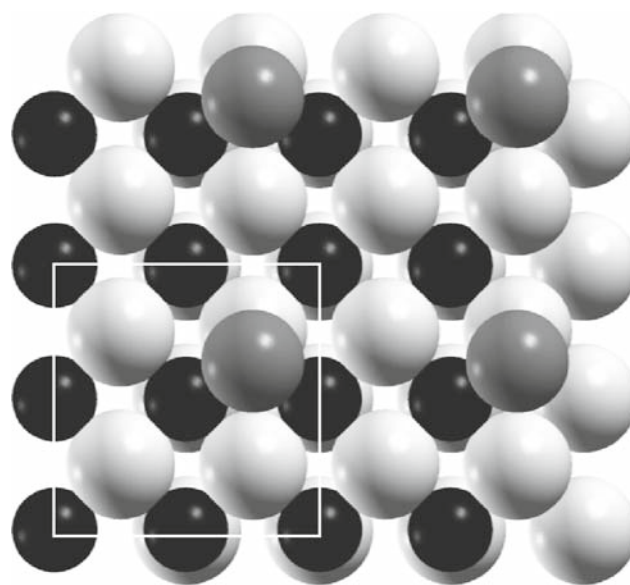
Fig. 1 Top view of a Au atom (grey sphere) adsorbed on the NiO(100) surface. Adsorption "on-top" of oxygen: the Au atom is tilted by 19° from the surface normal. *White spheres* oxygens, *black spheres* nickels. The *white square* shows the 2×2 supercell used

MgO(100) the adsorption on-top of oxygen, with a binding energy of 1.01 eV, comparable to that found here for NiO, is clearly preferred (but no tilt angle is found on MgO).

From these results it follows that Au atoms deposited on the NiO(100) surface should be able to diffuse almost freely along the surface even at very low temperature. In fact, the similar energies on the on-top and hollow sites indicate a very flat potential energy surface and suggest low diffusion barriers (not investigated here). The preference for Au to be displaced from the surface normal when it sits on oxygen is indicative of a direct interaction with Ni 3d states and of a covalent nature of the bond. In fact, it is the particular shape and orientation of the Ni $3d_{xz}$ or $3d_{yz}$ orbitals that leads to this specific bonding interaction. However, it should be noted that the tilting energy is small, and that the result could also be due to the particular treatment of d orbitals in DFT+U.
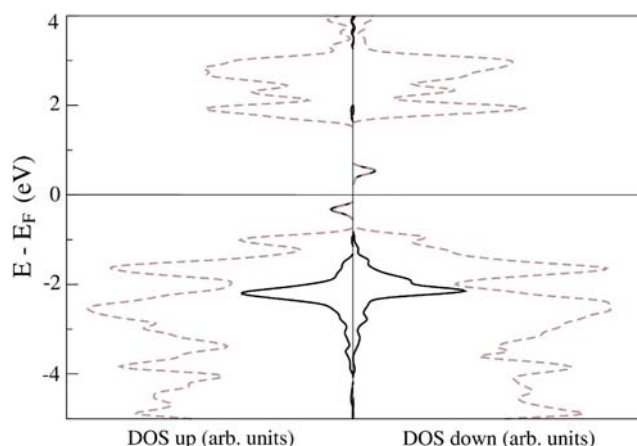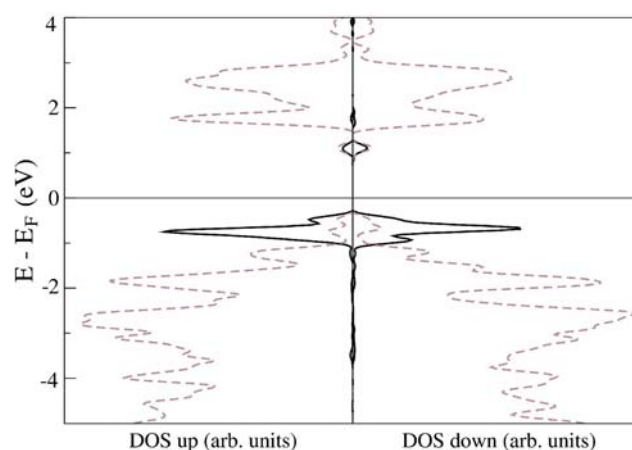
Fig. 2 Projected density of states of a gold atom adsorbed on the NiO(100) surface. *Dashed line* NiO. *Solid line* Au

Fig. 3 Projected density of states of a palladium atom adsorbed on the NiO(100) surface. *Dashed line* NiO. *Solid line* Pd

Fig. 4 Projected density of states of a platinum atom adsorbed on the NiO(100) surface. *Dashed line* NiO. *Solid line* Pt

The projected density of states (PDOS) of Au/NiO(100) is shown in Fig. 2. Despite the differences found with respect to the MgO surface, the DOS plot shows the same qualitative structure (see e.g. Fig. 5a in Ref. [42]). The Au 5d states are below the top of the O 2p band and the filled α component of the Au 6s level is about 1 eV above the top of the O 2p band. The corresponding β component is empty, above the Fermi level (E_F) so that one can conclude that, as on MgO(100), also on NiO(100) gold remains substantially neutral.
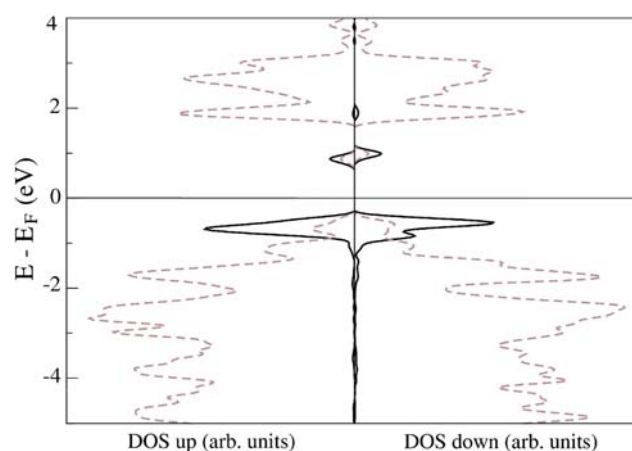
The second atom we considered is Pd which has a closed shell configuration [Kr]$5d^{10}6s^0$ and a much lower EA than Au (0.56 eV). As expected on the basis of the results for Pd adsorption on MgO [14], we found a strong bond when Pd is on-top of oxygen, 1.6 eV, (Table 1); the corresponding Pd–O distance, about 2.08 Å, is much shorter than for the Au case. Also in this case, however, the Pd atom is not exactly on-top of the surface anions but is tilted by about 16° from the surface normal. This result is quite similar to what observed on MgO, where the adsorption energies for O-top site is 1.56 eV. With respect to Au, we found that not only the potential energy surface is somewhat more corrugated, but also in this case low barriers for diffusion are expected. In fact, in hollow and Ni-top sites (constrained configurations), we found adsorption energies of 1.36 and 0.97 eV respectively.

The PDOS for Pd/NiO(100), Fig. 3, show that the Pd 4d states are at just above the O 2p valence band, but well below E_F. The Pd 5s state is empty, about 1 eV above E_F, which means that the Pd atom keeps the $4d^{10}$ electronic structure of the gas-phase atom. No net charge transfer occurs, and the changes in total electronic charge are those connected to the covalent mixing of the Pd and O 2p states.

The last atom considered is Pt. Pt belongs to the same group of Pd, but has a different electronic configuration, [Xe]$5d^96s^1$. It also has a rather large EA, 2.13 eV, only slightly smaller than that of gold. As we found for Au and Pd, only the tilted O-top site minimum exists, (Table 1). The Pt/NiO bond on the O-top site, 2.66 eV, is stronger than what observed for Au and Pd, and also the Pt–O distance, 1.98 Å, is the shortest, (Table 1). As for the other atoms, there is a tilt angle of about 18°. The stronger bonding of Pt is in line with previous extensive DFT studies of transition metal atoms adsorbed on MgO [43]. It was shown that Pd and Pt atoms form rather strong chemical bonds with the surface and that the trend of the binding energies is Pt > Pd > Au, showing a stronger covalent interaction between Pt and oxygen.

The PDOS curves of Pt on NiO(100) are shown in Fig. 4. The first remark is that the Pt DOS plot is very similar to that of Pd: the Pt 5d states are at the top of the valence band, while the 6s states are above the Fermi level (empty). This means that upon adsorption there is a change in electronic configuration from $5d^96s^1$ to close shell $5d^{10}6s^0$-like. This is also the reason for the formation of a strong bond. The Pt atom can in fact rearrange and transfer the 6s electron into the more contracted 5d shell, thus reducing the Pauli repulsion

and the distance from the surface. The consequence of this electronic redistribution is a spin quenching of the Pt atom which from a triplet configuration in gas-phase assumes a singlet one on the surface. On the other hand, no significant change in the magnetic moments of NiO is found upon Pt adsorption, as well as for the other adatoms considered.

To summarize the results of this section, the picture which emerges seems to indicate a clear preference of all the adsorbed atoms to bind to the anions, with a tilt angle with the respect of the surface normal. This tilt angle can be explained by the direct covalent interaction of the adatoms with Ni 3d states.

3.2 Adsorption of Au, Pd and Pt atoms on NiO/Ag(100)

We consider now the adsorption of the same atoms on 3L NiO films deposited on Ag(100). The interest here is to check wheather the interface bonding of the NiO slab to the Ag metal results in changes in adsorption properties or not.

The results of the adsorption of Au, Pd and Pt atoms on NiO/Ag(100) are summarized in Table 1. At first glance, one could think that significant changes occur when Au is adsorbed on the NiO/Ag(100) thin film compared to the NiO(100) surface. In fact, the O-top site is no longer the preferred site (the binding, about 0.85 eV, is slightly smaller than on NiO(100), 0.90 eV), and another minimum appears where the Au atom is in the hollow site, at variance with the NiO(100) results. Actually, the adsorption properties are only slightly different in the two cases, film and bare oxide. In the hollow site of NiO/Ag(100) the binding energy, 0.95 eV, is a bit larger than on the corresponding site of the bare surface (0.81 eV). The Ni-top site is only slightly higher in energy, 0.04 eV, and the Au atom forms a small tilt angle of 6° from the surface normal. This result might indicate the occurrence of a small charge transfer from the substrate to the adsorbed atom: this partial charge may be responsible for the change in adsorption site. The presence of the two minima, however, indicates once again the presence of a very flat energy potential.

The analysis of the PDOS curves for Au₁/NiO/Ag(100), Fig. 5, shows that the α component of the Au 6s level is occupied while the corresponding β component is almost empty and above the Fermi level (E_F). The small occupation of the β 6s Au state is confirmed by comparing the PDOS of the unsupported film (Fig. 2) with the corresponding PDOS of the supported one (Fig. 5): in the former case the two components of the 6s Au orbitals are separed by 0.1–0.2 eV, while in the latter case the Fermi level crosses the 6s β component. The description of the system is, however, very different from the case of Au adsorption on MgO/Ag(100) [20] or MgO/Mo(100) films [14], where the Au is a full anion and both components of the 6s Au levels are occupied below the Fermi level.
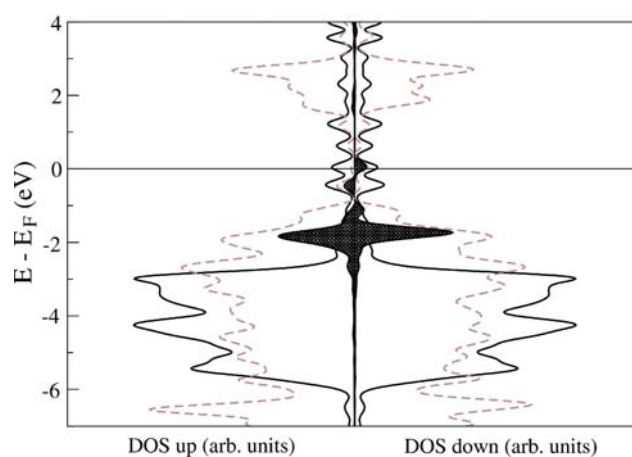
Fig. 5 Projected density of states of a gold atom adsorbed on the NiO/Ag(100) surface. *Solid line* Ag (3 uppermost layers). *Dashed line* NiO. *Black filled line* Au

Differently from the Au case, no significant differences are found in the adsorption properties of Pd and Pt deposited on NiO(100) or NiO/Ag(100): only the tilted O-top minimum is found and the binding energy is substantially the same, 1.60 eV and 1.58 eV for Pd, 2.66 eV and 2.63 eV for Pt, respectively (Table 1). Pt atom assumes a 5d¹⁰-like configuration and that the general characteristics of the bonding are the same discussed above for the NiO(100) surface. Also the distances and tilt angles are virtually the same in the two cases, showing that the presence of silver does not perturb the adsorption properties of the NiO(100) surface.

From these results we can conclude that the adsorption of Pd and Pt is very similar on NiO/Ag(100) films and on the NiO(100) surface. A minor difference is reported when Au is adsorbed on the NiO/Ag(100) film, where two minima are found on the hollow and Ni-top site. This behavior can be explained by the occurrence of a small charge transfer to the adsorbed Au atom. However, the extent of this charge transfer is definitely smaller than that observed on MgO/Ag(100) films. The reason for the different behavior is the different change in work function in the two systems, as it will be discussed in the next section.

3.3 Work function changes in multi-layer NiO-MgO films on Ag(100)

Oxide thin films may induce a significant changes in the work function of the metal support. In some cases this is related to the charge transfer at the interface between the oxide and the metal (this is the case of SiO₂ films, for instance [40]). In other cases, where no charge transfer occurs, like for TiO₂/Pt(111) films, the change in the work function of the system is negligible [44]. MgO films, on the contrary, induce a substantial work function change which is explained

with a polarization or "compression" effect, a mechanism of electrostatic nature [40,45]. The presence of the oxide layer reduces the amount of electronic charge that spills over from the metal surface, the metal electrons are polarized towards the surface, and the work function decreases [40]. In MgO/Ag(100) this reduction is of 1.2 eV and Φ converges to 3.2 eV (it is 4.3 eV on Ag(100), Table 2). Based on the same mechanism, for the NiO/Ag(100) interface one should expect an even stronger decrease of Φ. In fact, a linear correlation exists between interface distance and work function change (at least for MgO/metals [40]); in NiO/Ag(100) the interface distance is shorter than in MgO/Ag(100) [24], and the change in work function should be similar or even larger. On the contrary, the computed Φ for NiO/Ag(100) films is 3.9 eV, i.e., only 0.4 eV smaller than the clean Ag(100) surface [24]. At variance with the MgO surface, significant charge rearrangements occur at the NiO/Ag(100) interface: charge flows from the metal towards the Ni d(z^2) orbitals and at the same time the oxide anions transfer charge to the Ag substrate [24]. The global effect is a small reduction of the work function, much less pronounced than in the MgO/Ag(100) case. When Au is adsorbed on NiO/Ag(100), the Fermi level does not fall above the Au 6s level and only little charge transfer occurs.

In principle, one can think of possible ways to to "engineer" the oxide thin film so as to favor the occurrence of charge transfer from the metal substrate to an adsorbed atomic species. In order to do this one has to find ways to reduce the work function of the metal/oxide interface. We have seen above that MgO induces this effect due to the essentially electrostatic interaction with Ag(100) while NiO alters Φ only slightly because of an interface bond with more pronounced covalent character which cancels the compression effect. Since MgO and NiO have the same NaCl-like crystalline structure and very similar lattice parameters, one can in principle imagine a system where a thin MgO layer is deposited on Ag(100), so as to induce the large desired shift of Φ, and NiO is grown on top of this MgO layer so that the exposed surface is that of NiO. With modern techniques of chemical vapor or atomic layer deposition, such an interface
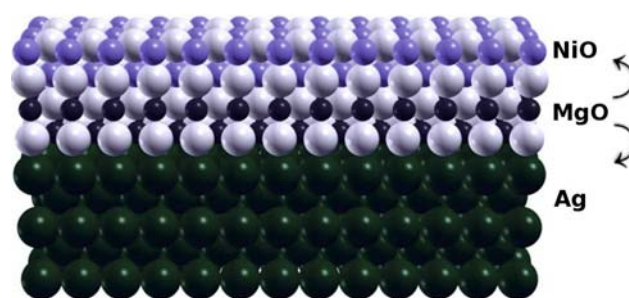
Fig. 6 Structure of a multi-layer NiO/MgO/Ag(100) film. The *arrows* indicate the directions of charge transfer from the MgO film to the Ag(100) substrate and to the NiO layer

could be realized in practice. If the entire film is sufficiently thin, <1 nm, tunneling can occur and spontaneous charging can take place to an adsorbed metal like gold.

To verify this hypothesis we have computed a multilayer oxide film composed of both NiO and MgO deposited on Ag(100), (Fig. 6), and determined the corresponding properties. We started by depositing 2L of NiO on a single MgO layer (Table 2). The properties of this system are very similar to those of the pure NiO 3L film: the interface distance is about 2.5 Å, the work function change is about −0.4 eV, and the adhesion energy, 25 meV/Å², is only slightly higher than for NiO(3L)/Ag(100). The absence of effect on the work function can be attributed to the fact that a single MgO layer is not thick enough to develop the typical ionic structure and insulating character of bulk MgO.

Thus, we have considered a new system where a MgO 2L film is placed between the NiO 2L slab and the Ag support. We found some of the typical properties of the MgO/Ag(100) interface: the separation becomes 2.7 Å as for a MgO 3L film while the adhesion energy, 13 meV/Å², is smaller than in MgO(3L)/Ag(100), (Table 2). However, the work function is 3.88 eV, with a reduction of only 0.41 eV with respect to the Ag(100) surface, practically the same value computed for NiO/Ag(100). What is the origin of this small work function change? A close look at the electronic structure reveals that the MgO intralayer donates a small amount of charge to the Ag support, 0.0040 and 0.0049 e/Å² for 1L and 2L cases,

Table 2 Comparison of interface properties of NiO/Ag(100), MgO/Ag(100), and mixed NiO/MgO/Ag(100) interfaces

		d (Å)	Φ (eV)	$\Delta\Phi$ (eV)	CT/S (e/Å²)(×10²)	E_{adh} (meV/Å²)
NiO(3L)/Ag(100)[a]	GGA+U	2.50	3.90	−0.39	−0.69	20
MgO(3L)/Ag(100)[b]	GGA	2.73	3.22	−1.07	0.47	23
NiO(2L)/MgO(1L)/Ag(100)	GGA+U	2.51	3.90	−0.39	0.40 (1.01)[c]	25
NiO(2L)/MgO(2L)/Ag(100)	GGA+U	2.72	3.88	−0.41	0.49 (1.04)[c]	13

nL number of layers, d interface distance, Φ work function, $\Delta\Phi$ work function change, $\Delta\Phi = \Phi[\text{Ag}(100)] - \Phi[\text{MO/Ag}(100)]$, CT/S charge transfer at the interface (positive from the oxide to the metal support), E_{adh} adhesion energy
[a] Results from Ref. [24]
[b] These results are slightly different from those reported in Ref. [24] because here we use the projected-augmented wave (PAW) approximation
[c] In parenthesis is the charge transfer from MgO to NiO

respectively, similar as in MgO/Ag(100) (Table 2). However, the MgO layer donates a larger amount of charge to the NiO film, about $0.010\,e/\text{Å}^2$, (Fig. 6, Table 2). This charge transfer leads to a surface dipole which has the effect to increase the work function. This contribution cancels almost entirely the compression effect of the MgO layer which acts to reduce the work function. The final result is that the global change is small, and not so different from that induced by a pure NiO layer.

To summarize, the use of a MgO layer as a buffer between NiO and Ag does not exhibit the expected effect to significantly reduce the work function because of charge transfers occurring at the oxide–oxide interface. The fact that the position of the Fermi level in NiO/MgO/Ag(100) multi-layer remains practically unchanged compared to NiO/Ag(100) suggests that the properties of transition metal atoms adsorbed on the two systems will be practically the same. For this reason we did not consider the problem explicitly.

4 Conclusions

The adsorption of transition metal atoms on the surface of NiO has been studied. The potential energy surface is rather flat, but in all the cases considered, the preferred adsorption site is roughly on top of the anion, with a tilt angle formed by the adsorbed atom with the surface normal. The strength of the interaction decreases in the order Pt > Pd > Au, as for adsorption on MgO. The bonding is dominated by covalent contributions. This holds true also for NiO ultra-thin films deposited on Ag(100). The adsorption properties are not very different from those of the NiO(100) surface. The only exception is represented by the Au atom, which prefers to bind on hollow and Ni-top sites. However, at variance with MgO/Ag(100) or MgO/Mo(100) ultra-thin films, no charge transfer (Pd and Pt) or a negligible charge transfer (Au) occurs from the metal substrate even to atoms with high electron affinities. The reason for this behavior is that the work function of NiO/Ag(100) is only $0.4\,\text{eV}$ smaller than that of the bare Ag(100) metal surface; on MgO/Ag(100), where charge transfer to deposited gold occurs, the change in work function is three times larger. For this reason we have designed new interfaces with MgO films at the interface and NiO films on top of it to exploit the characteristics of the individual oxide films to reduce the work function. However, charge transfer effects at the oxide–oxide interface cancels the effects of the MgO interface layer and result in moderate changes of the system work function.

References

1. Henry CR (1998) Surf Sci Rep 31:231
2. Bäumer M, Freund HJ (1999) Prog Surf Sci 61:127
3. Schmid G, Bäumle M, Geerkens M, Heim I, Osemann C, Sawitowski T (1999) Chem Soc Rev 28:179
4. Campbell CT (1997) Surf Sci Rep 27:1
5. Lambert RM, Pacchioni G (eds) (1997) Chemisorption and reactivity of supported clusters and thin films. NATO ASI Series E, vol 331, Kluwer, Dordrecht
6. Freund HJ (2002) Surf Sci 500:271
7. Abbet S, Sanchez A, Heiz U, Schneider WD, Ferrari AM, Pacchioni G, Rösch N (2000) J Am Chem Soc 122:3453
8. Judai K, Wörz A, Abbet S, Heiz U, Del Vitto A, Giordano L, Pacchioni G (2005) Phys Chem Chem Phys 7:955
9. Abbet S, Heiz U, Häkkinen H, Landman U (2001) Phys Rev Lett 86:5950
10. Frank M, Bäumer M (2000) Phys Chem Chem Phys 2:3723
11. Sterrer M, Risse T, Freund HJ, Carrasco J, Illas F, Di Valentin C, Giordano L, Pacchioni G (2006) Angew Chemie Int Ed 45:2633
12. Yulikov M, Sterrer M, Heyde M, Rust HP, Risse T, Freund HJ, Pacchioni G, Scagnelli A (2006) Phys Rev Lett 96:146804
13. Freund HJ (2007) Surf Sci 601:1438
14. Pacchioni G, Giordano L, Baistrocchi M (2005) Phys Rev Lett 94:226104
15. Ricci D, Bongiorno A, Pacchioni G, Landman U (2006) Phys Rev Lett 97:036106
16. Sterrer M, Risse T, Martinez Pozzoni U, Giordano L, Heyde M, Rust HP, Pacchioni G, Freund HJ (2007) Phys Rev Lett 98:096107
17. Kulawik M, Nilius N, Freund HJ (2006) Phys Rev Lett 96:036103
18. Sterrer M, Risse T, Heyde M, Rust HP, Freund HJ (2007) Phys Rev Lett 98:206103
19. Nilius N, Rienks EDL, Rust HP, Freund HJ (2005) Phys Rev Lett 95:066101
20. Giordano L, Pacchioni G (2006) Phys Chem Chem Phys 8:3335
21. Giordano L, Del Vitto A, Pacchioni G (2006) J Chem Phys 124: 034701
22. Baron M, Stacchionla D, Ulrich S, Nilius N, Shaikhoutdinov S, Freund HJ, Martinez U, Giordano L, Pacchioni G (2008) J Phys Chem C (in press)
23. Cococcioni M, De Gironcoli S (2005) Phys Rev B 71:035105
24. Cinquini F, Giordano L, Pacchioni G, Ferrari AM, Pisani C, Roetti C (2006) Phys Rev B 74:165403
25. Dovesi R, Saunders VR, Roetti C, Orlando R, Zicovich-Wilson CM, Pascale F, Civalleri B, Doll K, Harrison NM, Bush IJ, D'Arco P, Llunell P (2006) CRYSTAL06 User's Manual Università di Torino, Torino
26. Kresse G, Hafner J (1993) Phys Rev B 47:R558
27. Kresse G, Furthmüller J (1996) Phys Rev B 54:11169
28. Ferrari AM, Pisani C, Cinquini F, Giordano L, Pacchioni G (2007) J Chem Phys 127:174711
29. Anisimov VI, Zaanen J, Andersen OK (1991) Phys Rev B 44:943
30. Liechtenstein AI, Anisimov VI, Zaanen J (1995) Phys Rev B 52:R5467
31. Dudarev SL, Botton GA, Savrasov SY, Humphreys CJ, Sutton AP (1998) Phys Rev B 57:1505
32. Perdew JP, Chevary JA, Vosko SH, Jackson KA, Pederson MR, Singh DJ, Fiolhais C (1992) Phys Rev B 46:6671
33. Blöchl PE (1994) Phys Rev B 50:17953
34. Bengone O, Alouani M, Blöchl PE, Hugel J (2000) Phys Rev B 62:16392
35. Rohrbach A, Hafner J, Kresse G (2004) Phys Rev B 69:075413
36. Fender BEF, Jacobson AI (1968) J Chem Phys 48:990
37. Cheetham AK, Hope DAO (1983) Phys Rev B 27:6964
38. Sawatzky GA, Allen JW (1984) Phys Rev Lett 53:2339
39. Fujimori A, Minami F (1984) Phys Rev B 30:957

40. Giordano L, Cinquini F, Pacchioni G (2005) Phys Rev B 73: 045414
41. Wörz AS, Heiz U, Cinquini F, Pacchioni G (2005) J Phy Chem B 109:18418
42. Giordano L, Baistrocchi M, Pacchioni G (2005) Phys Rev B 72: 115403
43. Yudanov I, Pacchioni G, Neyman K, Rösch N (1997) J Phys Chem 101:2786
44. Zhang Y, Giordano L, Pacchioni G, Vittadini A, Sedona F, Finetti P, Granozzi G (2007) Surf Sci 601:3488
45. Goniakowski J, Noguera C (2004) Interface Sci 12:93